

## THE SOUTHERN SKY REDSHIFT SURVEY

L. NICOLACI DA COSTA AND P. S. PELLEGRINI  
 Departamento de Astronomia, CNPq/Observatorio Nacional

W. L. W. SARGENT AND J. TONRY  
 California Institute of Technology

M. DAVIS AND A. MEIKSIN  
 Departments of Physics and Astronomy, UC Berkeley

DAVID W. LATHAM  
 Harvard-Smithsonian Center for Astrophysics

AND

J. W. MENZIES AND I. A. COULSON  
 South African Astronomical Observatory

### ABSTRACT

We have finished a redshift survey of galaxies selected from the ESO catalog and present here maps of the resulting space distribution. The sample consists of 2028 galaxies in an area of 1.75 sr with declination south of  $-17^{\circ}.5$  and galactic latitude below  $-30^{\circ}$ . The sample diameter is limited with all galaxies having  $\log [D(0)]$  greater than 0.1 where  $D(0)$  is a “face-on” diameter in arcminutes. The redshift sample is not complete at the smallest diameter, particularly for the later type galaxies, for which the surface brightness is very low; redshifts are available for 1657 of the galaxies. This survey provides useful information on large-scale structure to a depth of  $120 h^{-1}$  Mpc ( $H_0 = 100 h \text{ km s}^{-1} \text{ Mpc}^{-1}$ ). The galaxy distribution exhibits prominent filaments, sheets, and voids as seen in previous surveys, although there are no very rich clusters within the sample, the observed structure displays a diverse heterogeneity of morphology; some large-scale structures are highly sub-clustered, others are much more diffuse. Only a few of the more compact groups display conspicuous redshift space distortion. One large void in the foreground has an extent of  $20 \times 30 \times 50 h^{-1}$  Mpc and appears quite promising for future searches of material less clustered than luminous galaxies.

*Subject headings:* cosmology — galaxies: clustering — galaxies: redshifts

### I. INTRODUCTION

In recent years considerable progress has been made in the observational study of the space distribution of galaxies. In particular, over the past decade several large-scale redshift surveys have led to a dramatic change in our ideas of the clustering pattern of galaxies in the universe (see the review by Huchra and Geller [1987] for a summary of recent surveys). It is now recognized that the distribution of galaxies is very inhomogeneous, with galaxies tending to concentrate in high-density clusters and lower density filaments and sheetlike structures that pervade space, delineating large empty regions largely devoid of bright galaxies. Although some properties of the distribution, such as the statistics derived from the two-point correlation function,  $\xi(r)$ , are thought to be well determined on small scales ( $r < 5 h^{-1}$  Mpc), even the sign of  $\xi(r)$  is undetermined for  $r > 15 h^{-1}$  Mpc, and the overall pattern of the galaxy distribution is still controversial. This results from the heterogeneity and complexity of the observed structure on large scale; the volumes surveyed thus far are too small to be confident that they are sufficiently representative. Some sections of the universe appear remarkably ordered, with a large fraction of the galaxies readily associated with well-defined filaments (see, e.g., de Lapparent, Geller, and Huchra 1986), while other sections appear chaotic and disordered, with no obvious clustering centers (e.g., several sections from Davis *et al.* [1982] and Haynes and Giovanelli [1986]). The study of the topology of the galaxy distribution and the geometrical properties of individual large-scale structures is further compli-

cated by the expected distortions in the redshift maps used to represent the actual three-dimensional distribution of galaxies (Kaiser 1987).

The topological information is of great interest since different scenarios for the formation of large-scale structures probably lead to different topologies of the galaxy distribution. Both the hot dark matter and cold dark matter models are fully specified by their initial power spectra of density perturbations because the initial perturbations are expected to have had random phases, leading to Gaussian random initial fluctuations. These two models with rather different initial spectra seem to lead to virtually identical topologies as defined by Gott, Melott, and Dickinson (1986). However, the nonrandom phase models, such as the explosion models (Ostriker and Cowie 1981; Ostriker, Thompson, and Witten 1986) wherein large bubbles form hydrodynamically around isolated rare events, are likely to have somewhat different topology today. The cosmic string model is another example where the fluctuations are initially non-Gaussian, and the present topology of structures in this model should also differ from the Gaussian models.

The largest existing complete redshift survey is the original CfA survey (Huchra *et al.* 1983) which is a wide-angle modest depth survey claimed, by at least some of its authors, to possibly represent a fair sample of the universe at large. In the past few years this sample has been used extensively in a variety of statistical analyses and to confront the results of theoretical  $N$ -body models for the formation and evolution of structures

in the universe. However, as pointed out by Davis *et al.* (1982) and by Davis and Huchra (1982, hereafter DH), the largest structures observed are comparable in size to the survey depth, casting some doubt on how representative of the universe this sample is on scales larger than  $20 h^{-1}$  Mpc. Since its completion there has been considerable interest in extending the original CfA survey both in depth and in sky coverage. For the past 5 yr, several groups have followed these two routes (da Costa *et al.* 1984; de Lapparent, Geller, and Huchra 1986; Menzies, Coulson, and Sargent 1987). The southern extension of the CfA redshift survey is of particular interest since it probes a different and, perhaps, more representative region of space that avoids the large concentration of galaxies associated with the Virgo cluster. At the same time it provides the first expanded view of our surroundings to the south. Furthermore, another large survey can be used to address the question of the statistical reproducibility of the results obtained in the original CfA survey. These considerations have motivated a cooperative effort of several groups to complete a survey of over 2000 galaxies, here referred to as the Southern Sky Redshift Survey (SSRS), covering an area of 1.75 sr of the south Galactic cap in the region south of declination  $-17^{\circ}5$  and below galactic latitude  $-30^{\circ}$ . The goal was to obtain a complete sample down to a limiting galactic diameter given by  $\log [D(0)] = 0.1$ , where  $D(0)$  is in arcminutes. In this paper we present redshift maps of the observed galaxy distribution and a qualitative description of the nature of the galaxy clustering. In § II we describe the properties of the selected southern sample, while in § III we show different projection maps of the galaxy distribution and describe the main features observed. Finally, in § IV the general characteristics of the three-dimensional distribution of galaxies are discussed. A future paper will discuss more quantitative aspects of the statistics of the galaxy distribution.

## II. GALAXY DATA

The sample of galaxies was selected from the ESO/Uppsala catalog (Lauberts 1982) which is considered complete for galaxies south of declination  $-17^{\circ}5$  with major diameters greater than  $1'$ . The information on morphological types and the values of the major and minor diameters for each galaxy were used to define a diameter-limited catalog based on a "face-on" diameter  $D(0)$  defined by the expressions

$$\log [D(0)] = \log (D_1) - 0.235A(T) \log (D_1/D_2), \quad (1)$$

where

$$\begin{aligned} A(T) &= 0.894 & T > 0 \\ &= 0.950 & T < 0. \end{aligned} \quad (2)$$

In these equations  $D_1$  and  $D_2$  are the major and minor diameters and  $T$  denotes the morphological type as listed in the ESO/Uppsala catalog. We note that the above definition of  $D(0)$  is similar but not identical to that given by de Vaucouleurs, de Vaucouleurs, and Corwin (1976, hereafter RC2), since no correction is made for the major diameter to transform it to the isophotal system used in the RC2. In addition, the correction for the axial ratios is assumed to be similar to that determined in the RC2 for the axial ratios given by the Uppsala General Catalog (UGC, Nilson 1973). We emphasize that for the definition of a statistical sample it is not important to define an absolute system but simply to have a well-defined criterion in order to correct for selection effects, in the same way as is usually done for magnitude-limited samples. The diameter cutoff was arbitrarily chosen to be  $\log [D(0)]_{\text{lim}} = 0.1$ .

Adopting this diameter limit we have drawn 2028 objects over an area of 1.75 sr, within the region defined by galactic latitude below  $-30^{\circ}$  and declination south of  $-17^{\circ}5$ , corresponding to a mean surface density of 1159 galaxies per steradian. This value is comparable to the mean surface density of galaxies in the magnitude-limited sample of the northern Galactic cap of the CfA survey, which includes the Virgo cluster. Therefore we find that using the diameter limit defined above we should sample at least as deep as the northern survey if not somewhat deeper.

Although a diameter-limited catalog is a perfectly valid statistical sample and in some applications may even be superior, it is important to note that it yields a quite different sample from one selected in terms of a limiting magnitude. In particular, it leads to a relative increase of low surface brightness (LSB) galaxies which makes completeness of the optical spectroscopy difficult. For example, selecting a diameter-limited sample from the Nilson UGC catalog (1973) yields 7% ellipticals, 12% lenticulars, 61% spirals, 2% irregulars, 8% dwarfs, and 8% others. In a magnitude-limited selection of the same UGC catalog, Davis and Geller (1976) found 10% ellipticals, 17% lenticulars, 55% spirals, 5% irregulars, 0.4% dwarfs, and 15% others, i.e., essentially no dwarfs. In the ESO diameter-limited sample there are 3% ellipticals, 17% lenticulars, 63% spirals, 8% irregulars, 7% dwarfs, and 2% others. Apparently the E/S0 division is not consistent between ESO and UGC, but otherwise the distributions are similar. It appears that a diameter-limited catalog yields a dramatic increase in the fraction of dwarfs, and a relative decrease in high surface brightness early-type galaxies when compared to a magnitude-limited sample. This is not unexpected.

The original sample of 2028 objects selected from the diameter cutoff chosen includes several multiple systems and interacting galaxies (IGs) as defined in the classification scheme adopted by Lauberts (1982). Since a single diameter has been quoted for these systems we have examined these cases individually in order to determine whether each member galaxy met the selection criterion, in which case they were assigned morphological types, diameters, and new coordinates. All 170 IG entries, including 30 multiple systems and 140 binary or perturbed galaxies, were examined using the ESO (B) and ESO/SRC on-film copies. From the plate inspection, all galaxies in IG systems, but with diameters below our cutoff, were excised from the list, leaving a total of 1963 individual galaxies.

Radial velocities for the galaxies in the sample were obtained in a collaborative effort with observations being made at the Observatorio Nacional (ON), Las Campanas Observatory (LCO), and South African Astronomical Observatory (SAAO). The data and a discussion of the quality of the radial velocities are presented elsewhere (da Costa *et al.* 1984; Menzies, Coulson, and Sargent 1987; Sargent *et al.* 1987). The velocities from all three groups are of high quality with an estimated error of less than  $40 \text{ km s}^{-1}$ . A substantial fraction of the sample has at least two and sometimes three redshift measurements which allows a good intercomparison among the different sets of observations. A final catalog which consolidates all the available data will be compiled in the near future (Sargent *et al.* 1987).

Combining all the observations we have radial velocities for a total of 1657 galaxies. The remaining objects had too low a surface brightness to allow the measurement of an optical redshift in the time available. This means that our completeness is not an exact step function of  $D(0)$ , and corrections should be made to account for this effect which is, in general, a function

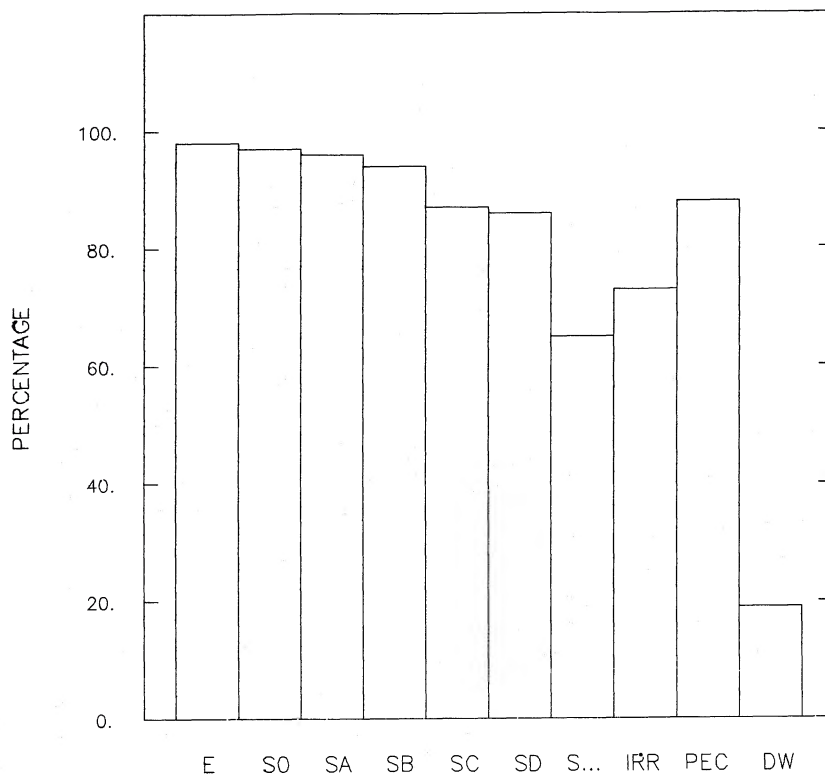


FIG. 1.—The completeness of the SSRS sample as a function of the morphological type

of the morphological type, as shown in Figure 1. Our completeness rate is high up to Sc falling dramatically for later types or unclassified galaxies. The sample of dwarfs is especially incomplete since very little radio data are available in the southern hemisphere, and it is very difficult to obtain an optical redshift in reasonable integration times for low surface brightness galaxies. The incompleteness as a function of  $D(0)$  for different morphological type groups is shown in Figure 2, and it is clear that the corrections amount to less than 20%, except for Sd, Irr, and dwarf galaxies. Although the plots shown below include the dwarfs, these were discarded from the quantitative analysis below, which considers a sample of 1830 galaxies with a redshift completeness of 90%.

### III. GALAXY DISTRIBUTION

#### a) Space Density

Since we are dealing with a diameter-limited sample, at increasingly larger distances only the intrinsically larger galaxies will make it into the catalog. This introduces a selection effect that must be taken into account in any statistical analysis. In a similar fashion, when dealing with a magnitude-limited sample we may define a selection function  $\phi(r)$  to be the fraction of galaxies at distance  $r$  that are sufficiently large to be included in the catalog. The derivation of this selection function is entirely analogous to that adopted by DH in the analysis of the CfA sample. It is derived from the ratio of the number of galaxies whose maximum observable distance is between  $r$  and  $r + dr$  to the number of galaxies within a distance  $r$  observable to distances greater than or equal to  $r$ . The incompleteness of the present redshift sample presents only minor difficulties which are not relevant to the largely qualita-

tive discussion below. A more detailed analysis will be presented elsewhere.

In order to minimize selection effects and to allow a comparison with the results of DH we have also defined a semivolume-limited sample, deleting galaxies that are not observable to at least a distance corresponding to  $4000 \text{ km s}^{-1}$ , resulting in a sample of about 1236 galaxies with absolute physical diameters  $D$  greater than  $14.6 h^{-1} \text{ kpc}$ . For the semivolume-limited sample the selection function is, by definition, unity for  $r$  less than  $40 h^{-1} \text{ Mpc}$ , decreasing steeply with distance beyond that, as shown in Figure 3. We recall that we do not include in our analysis the dwarf galaxies. This should not matter since most dwarf galaxies are likely to be nearby, intrinsically small galaxies and thus will be rejected from the semivolume-limited survey. For comparison Figure 3 also shows the selection function computed for the CfA northern cap sample, assuming a  $250 \text{ km s}^{-1}$  Virgocentric infall velocity. Note that, as expected, the diameter-limited sample extends somewhat deeper than the CfA sample; the maximum distance at which this sample can be considered statistically useful [ $\phi(r) = 0.1$ ] is approximately  $90 h^{-1} \text{ Mpc}$  compared to  $75 h^{-1} \text{ Mpc}$  for the CfA sample.

The definition of the selection function allows one to determine an unbiased estimate of the mean number density of galaxies with diameters greater than  $14.6 h^{-1} \text{ kpc}$ . We have evaluated the mean density utilizing the estimator  $n_1$  defined by DH,

$$n_1 = \frac{1}{V} \sum_{\text{shells}} \frac{N_c(r)}{\phi(r)} = 6.51 \times 10^{-3} \text{ galaxies Mpc}^{-3}. \quad (3)$$

In the above equation  $N_c(r)$  is the number of observed galaxies in the radial interval  $dr$  at a distance  $r$ . The volume  $V$  and the

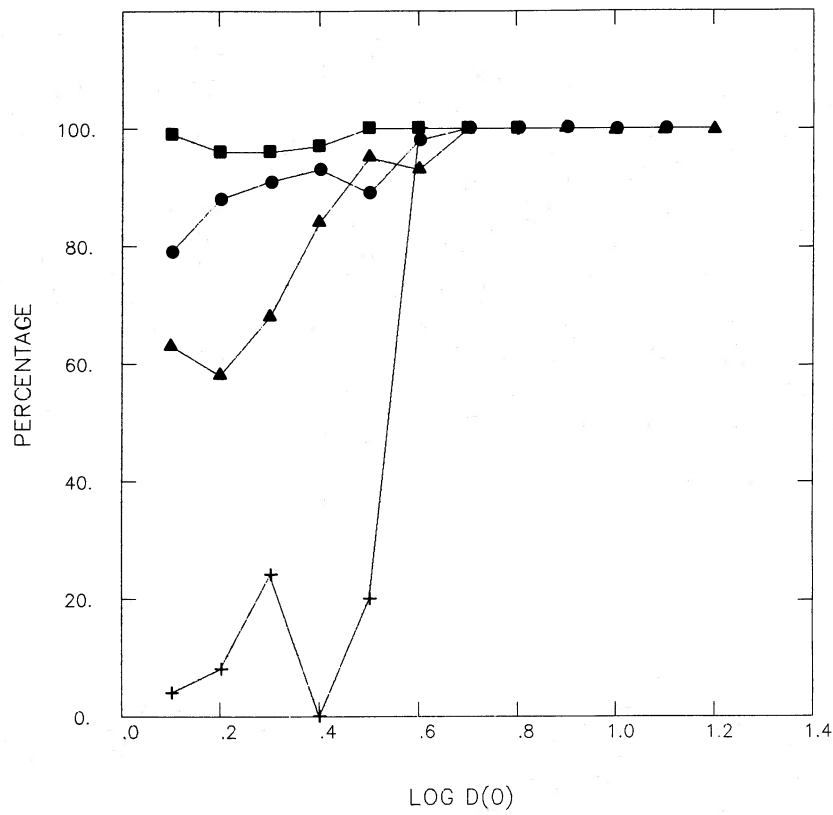


FIG. 2.—The completeness of the SSRS sample as a function of the “face-on” diameter  $D(0)$ , for different morphological type groups. The different symbols denote *full squares*: early-type galaxies; *open circles*: spirals; *full triangles*: Sd and Irregulars; *crosses*: dwarfs.

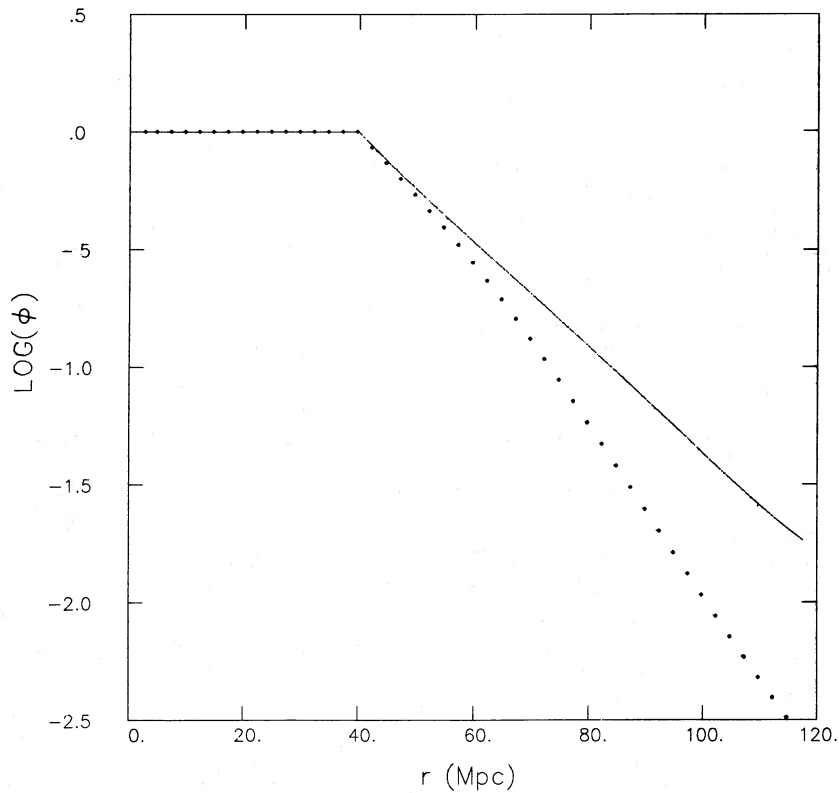


FIG. 3.—Comparison between the selection functions for volume-limited samples for the southern (*continuous line*) and northern hemispheres (*dotted line*). The southern sample is the diameter-limited sample of the SSRS, while the northern is the CfA one, both volume-limited at  $4000 \text{ km s}^{-1}$ . The curves were derived assuming a Virgocentric infall of  $250 \text{ km s}^{-1}$ .

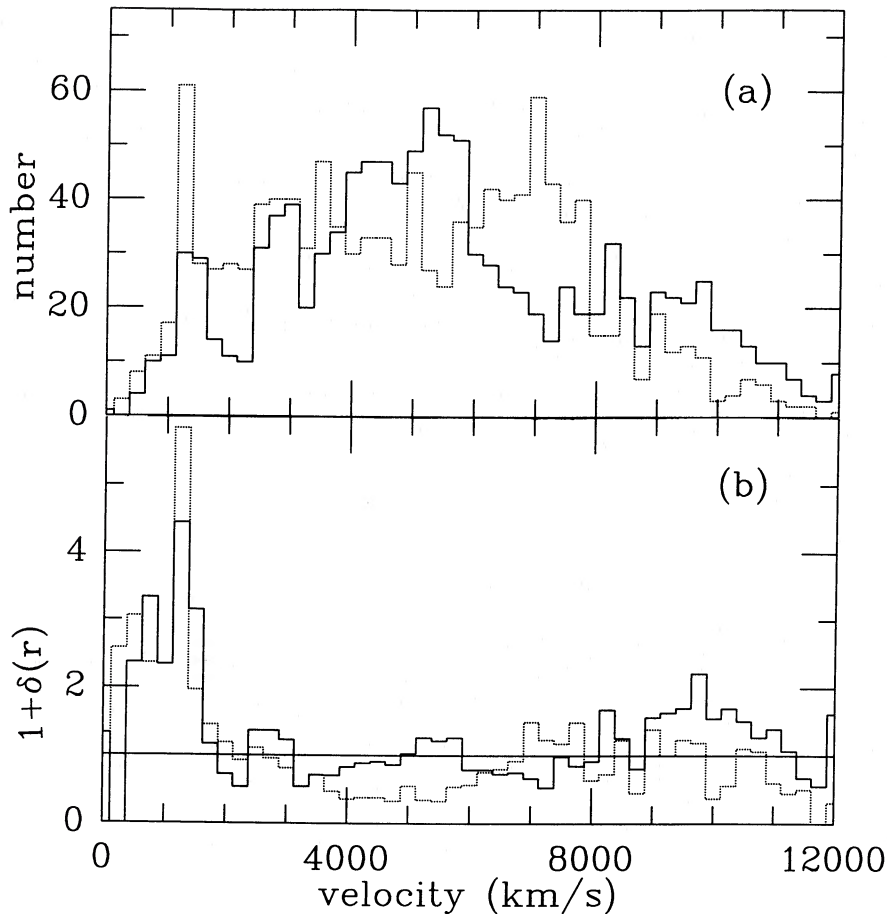


FIG. 4.—(a) Histogram of the observed counts of galaxies per shell of width  $250 \text{ km s}^{-1}$ ,  $N_c$ , in the SSRS (continuous line) and the CFA north (dotted line) samples. Only galaxies in the semivolume-limited subset are included. (b) Histogram of the overdensity in shells  $1 + \delta(r) = N_c/N_e$  for the two samples.

summation have been cut off at  $90 h^{-1} \text{ Mpc}$ . Velocities were corrected for a spherical infall of  $250 \text{ km s}^{-1}$  for the Local Group toward Virgo. Unfortunately, the different selection criteria between the northern and southern surveys prevents an accurate comparison of the mean densities of the two surveys, which would be the best indicator of the “fairness” of either sample. Hopefully this important comparison will be possible once magnitudes are available for the ESO catalog.

While the absolute value of  $n_1$  cannot be directly compared with the CfA result (for galaxies brighter than  $M_B = -18.5$ ) we may use the mean values calculated for both samples to examine the radial variation of the overdensity in the north and the south as shown in Figure 4. Figure 4a plots the raw distribution of counts per bin of width  $250 \text{ km s}^{-1}$ ,  $N_c$ , for galaxies in the semivolume-limited distribution in the two surveys after correcting the observed velocity for Virgocentric infall. This distribution should be relatively unaffected by the incompleteness of our redshift survey because few of the missing galaxies are likely to have sufficient intrinsic size to be in the semivolume-limited subset. Figure 4b is the histogram of  $N_c$  divided by the number of counts per bin,  $N_e$ , expected if the galaxies were homogeneously distributed with density  $n_1$ .  $N_e$  is given simply by  $N_e = \omega \phi(r) r^2 dr$  where  $\omega$  is the solid angle of the survey.

The similarities in Figure 4b between the two surveys are striking, including the presence of nearby clusters in both

hemispheres followed by underdense regions. The mean underdensity of the hole in the region  $3000 < v < 6000 \text{ km s}^{-1}$  is quite substantial for the northern survey, and there is nothing quite as dramatic in the south. The close agreement in overdensity contrast of foreground clusters of the north and the south is a cause for concern, as the Virgo supercluster in the north is certainly richer than Fornax plus Eridanus in the south, all of which are prominent in the magnitude-limited Shapley-Ames catalog. A complete set of magnitudes will we hope, clear up this mystery, which could be caused by nonlinearities in the ESO diameter scale.

#### b) Space Distribution

In Figure 5a we plot the distribution of all galaxies in our diameter-limited sample (1963 galaxies), including those without measured redshifts, projected onto the sky in equal area galactic coordinates. The most noticeable feature of this distribution is the enhanced structure along the north-south direction in the range  $\alpha = 3^{\text{h}}\text{--}4^{\text{h}}$ . A less concentrated structure runs across the sky along the east-west direction from  $\alpha = 0^{\text{h}}$  to  $\alpha = 3^{\text{h}}$ . A V-shaped structure with sides aligned preferentially along the north-south direction occupies the region between  $\alpha = 20^{\text{h}}$  and  $22^{\text{h}}$ . Redshift information shows the filamentary appearance of these structures to be real in most cases. In Figure 5b we present the projected distribution of galaxies lacking redshifts. These are mostly dwarfs, which to a large

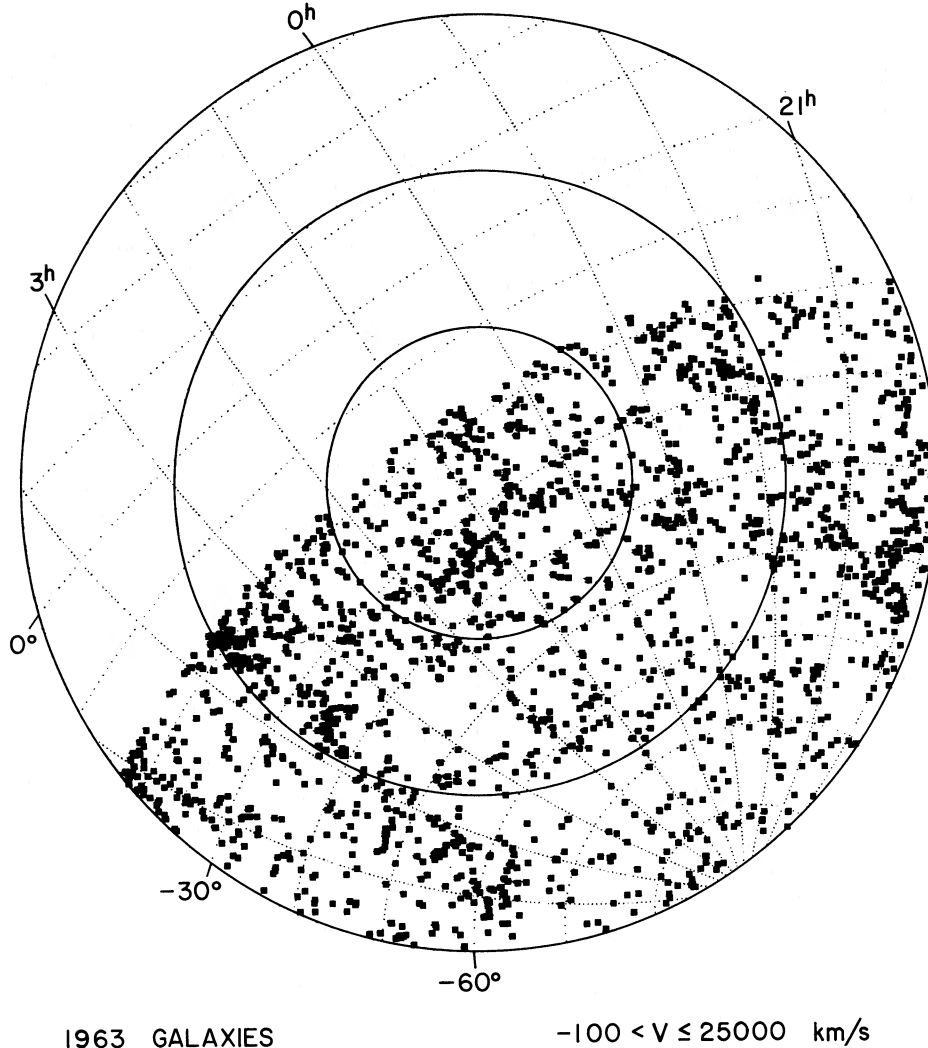


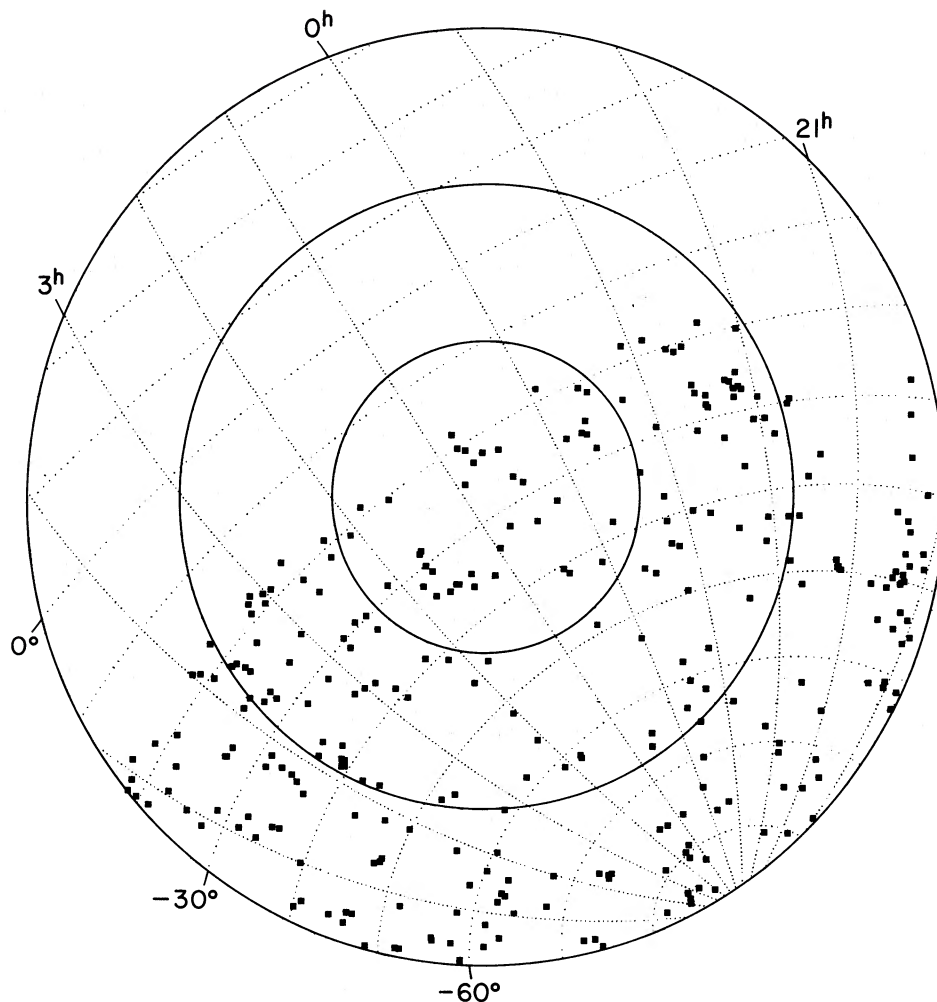
FIG. 5a

FIG. 5.—The 1963 galaxies of the SSRS sample (a) and the subset of 296 galaxies without measured velocities (b) projected onto equal area galactic coordinates. The south galactic pole is at the center and the circles denote the galactic latitudes  $-70^\circ$ ,  $-50^\circ$ , and  $-30^\circ$ . In the plot, constant declination and right ascension are indicated by dotted lines. About 200 of the galaxies without redshifts are either unclassified spirals or types later than Sc, of which 107 are dwarfs.

extent, follow the same general pattern displayed in Figure 5a. This indicates that the neglect of the dwarfs and other low surface brightness galaxies without measured redshifts should not hamper any future statistical analysis.

We examine the space distribution of all the observed galaxies by presenting in Figure 6 the data in distinct redshift windows. The nearest window is artificially richer than the others since it includes nearby intrinsically small galaxies. In the first window ( $0 < v < 3000 \text{ km s}^{-1}$ ) the most prominent structures are the Fornax cluster ( $3^{\text{h}}5$ ,  $-35^\circ$ ,  $1100 \text{ km s}^{-1}$ ) and the Eridanus group ( $3^{\text{h}}5$ ,  $-21^\circ$ ,  $1320 \text{ km s}^{-1}$ ) at the northern edge of the survey area. These two systems seem to form, with the looser group in Dorado ( $4^{\text{h}}5$ ,  $-58^\circ$ ,  $810 \text{ km s}^{-1}$ ), a connected linear structure that may extend beyond the present boundary of the survey. There are also two clearly discernible low-density regions suggesting the presence of two nearby voids: void 1 located approximately between right ascensions  $0^{\text{h}}$  and  $3^{\text{h}}$  and between declinations  $-40^\circ$  and  $-60^\circ$ , and void 2 located around  $\alpha = 21^{\text{h}}$  and  $\delta = -25^\circ$ . Other recognizable

high-density structures in this redshift window are several well-known nearby groups of galaxies like the Grus group ( $23^{\text{h}}$ ,  $-39^\circ$ ,  $1390 \text{ km s}^{-1}$ ), the NGC 7213 group ( $22^{\text{h}}2$ ,  $-46^\circ$ ,  $1800 \text{ km s}^{-1}$ ), and NGC 7144 group ( $21^{\text{h}}9$ ,  $-49^\circ$ ,  $1650 \text{ km s}^{-1}$ ) all listed in previous group catalogs (de Vaucouleurs 1975; Sandage 1975; Huchra and Geller 1982). This concentration of groups in the range  $\alpha = 21^{\text{h}}$  to  $23^{\text{h}}$  seems to be the front end of a large-scale structure stretching some  $4000 \text{ km s}^{-1}$  in depth. The main part of this structure, the so-called Telescopium-Pavo-Indus complex, can be seen in the second redshift window (Fig. 6b) which shows the velocity interval  $3000 < v < 6000 \text{ km s}^{-1}$ . It has a well-defined filamentary appearance and extends over  $40^\circ$  across the sky at the western section of the surveyed area. This filament delineates a third void (void 3) centered around  $\alpha = 23^{\text{h}}5$  and  $\delta = -35^\circ$ . The other low-density region between  $\alpha = 0^{\text{h}}$  and  $4^{\text{h}}$  and  $\delta < -45^\circ$  is a continuation of void 1. In this velocity interval we also see a large structure with a nearly uniform surface density of galaxies covering an area of roughly 600 square degrees centered



296 GALAXIES

FIG. 5b

at  $\alpha = 2^{\text{h}}$  and  $\delta = -30^{\circ}$ . This loose structure is in fact a flattened distribution seen here nearly face-on. In Figures 7a-c below this feature is a prominent diagonal structure stretching over  $50 h^{-1}$  Mpc, from ( $4^{\text{h}}5$ ,  $4000 \text{ km s}^{-1}$ ) to ( $0^{\text{h}}5$ ,  $9000 \text{ km s}^{-1}$ )! This feature has not been previously noted, and we shall refer to it as the “wall.”

In Figure 6c we show the redshift window  $6000 < v < 10,000 \text{ km s}^{-1}$  where the galaxies exhibit a trend to concentrate in the middle section of the plot in the range  $0^{\text{h}} < \alpha < 2^{\text{h}}$  separating what appears to be two low-density regions. The westernmost, in the range  $\alpha = 21^{\text{h}}-0^{\text{h}}$  is the extension of void 3, while the other centered at approximately  $\alpha = 4^{\text{h}}$  and  $\delta = -40^{\circ}$  and covering two hours of right ascension, is the fourth (void 4) very low density region that can be identified on the basis of these maps. Additional discussion of these empty regions is given below. Finally, Figure 6d shows the distribution of galaxies beyond  $10,000 \text{ km s}^{-1}$ . While a substantial number of galaxies have been observed with  $v > 10,000 \text{ km s}^{-1}$ , at these large distances the distribution is severely under-sampled with only the largest galaxies being surveyed, preventing any attempt to describe in a meaningful way the characteristics of the sample at these distances.

A more convenient way of showing the characteristics of the three-dimensional galaxy distribution is provided by the wedge diagrams shown in Figure 7, where we plot right ascension versus redshift, for different declination slices. We present only galaxies up to  $12,000 \text{ km s}^{-1}$  and use different symbols to denote different morphological type groups, as described in the figure captions. While a detailed description of the spatial distribution is a difficult task akin to detailing cloud formations in the sky, the basic feature of these maps that stands out immediately is the high degree of clustering exhibited by the galaxies. Large-scale linear and apparently connected structures delineate large empty regions. Although different in detail, the observed distribution clearly resembles those of previous surveys. One interesting characteristic of the present sample is the lack of prominent clusters in the surveyed volume. Redshift distortion effects are conspicuous only as mild radial elongations in the foreground groups. In general, the large-scale structures detected in the present survey cut across the line of sight and thus cannot be mistaken for “finger of god” structures due to virial motion within individual clumps.

In the foreground of Figures 7a-c the Fornax and Eridanus clusters are prominent; the signal-to-noise ratio on these clus-

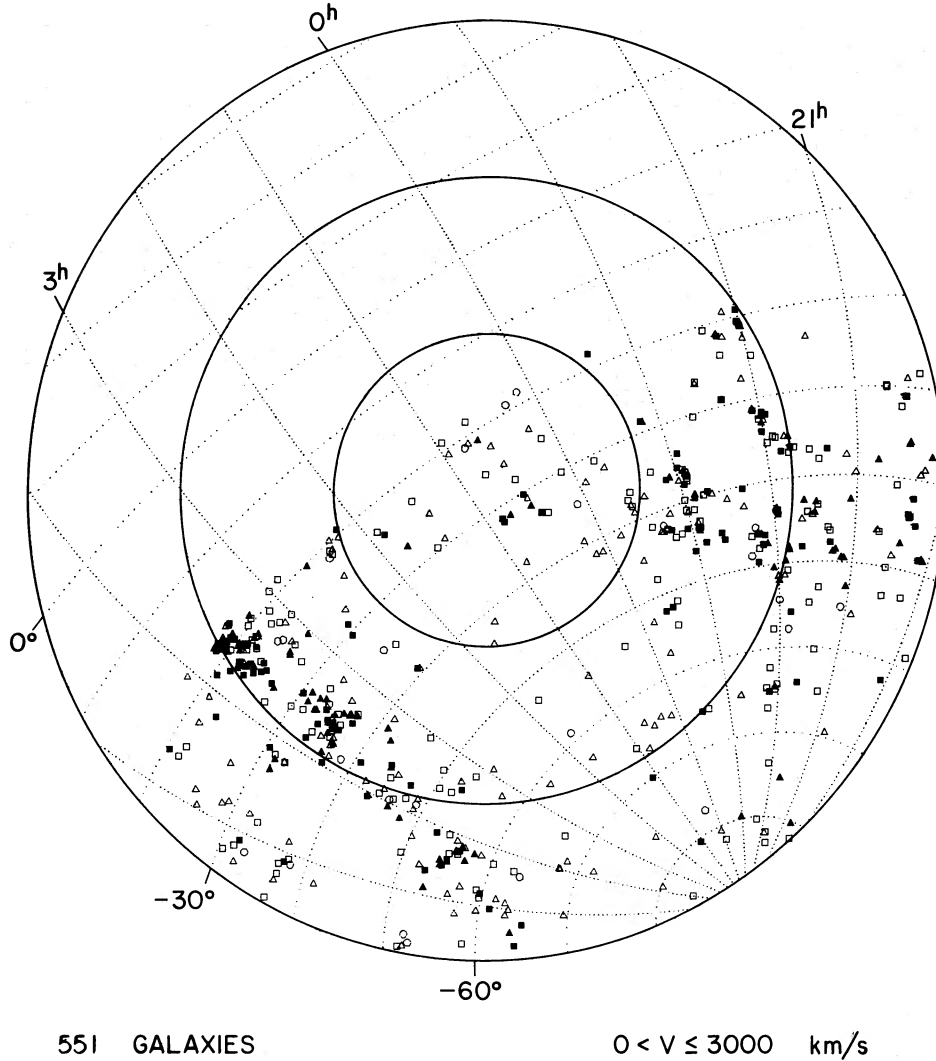


FIG. 6a

FIG. 6.—Projected distribution of galaxies, for different redshift windows, in the same coordinates as in Figure 5. The various symbols denote different morphological type groups: *full triangles*: E and S0; *full squares*: Sa and Sb; *open squares*: Sc; *open triangles*: unclassified spirals, peculiar, and irregular galaxies; *open circles*: dwarf galaxies.

ters and surrounding voids is best because the diameter function is probed most deeply. As a consequence it is possible to discern relatively sharp transitions between high- and low-density zones. In the region of  $20^{\text{h}}\text{--}21^{\text{h}}$  the distribution is dominated by an elongated structure, the Telescopium-Pavo-Indus clouds. These must be distinct structures as there is a gap from  $3000$  to  $4000 \text{ km s}^{-1}$  in this complex. The most prominent structure in the middle region of the map is the long diagonal filament, the “wall” mentioned above. This structure is of low-density contrast and is approximately  $50 \times 20 \times 10 h^{-1} \text{ Mpc}$  in extent. Note in all these maps that the different morphological types appear quite mixed throughout the structures; no obvious morphological segregation is apparent in the maps, an impression confirmed by correlation analysis.

Several low-density void regions are also conspicuous in the wedge diagrams. We summarize their positions and provide rough estimates of their sizes in Table 1. Perhaps the best defined void because of its proximity is void 1, located in the

foreground just behind the Eridanus-Fornax-Dorado complex, with a mean redshift of approximately  $3000 \text{ km s}^{-1}$  and between  $\alpha = 0^{\text{h}}$  to the easternmost limit of the survey. In the wedge diagrams it clearly extends through all observed slices, and is especially well defined south of  $\delta = -30^\circ$ . Since it is at

TABLE 1  
SSRS VOIDS

Void	Center	Dimensions ( $h^{-1} \text{ Mpc}$ )
1.....	$\alpha = 1^{\text{h}5}, \delta = -50^\circ$ $z = 3000 \text{ km s}^{-1}$	$z \Delta\alpha \sim 30, z \Delta\delta > 30, \Delta z \sim 40$
2.....	$\alpha = 21^{\text{h}}, \delta = -25^\circ$ $z = 5000 \text{ km s}^{-1}$	$z \Delta\alpha > 30, z \Delta\delta \sim 30, \Delta z \sim 30$
3.....	$\alpha = 23^{\text{h}5}, \delta = -35^\circ$ $z = 6000 \text{ km s}^{-1}$	$z \Delta\alpha \sim 70, z \Delta\delta \sim 30, \Delta z \sim 50$
4.....	$\alpha = 4^{\text{h}}, \delta = -40^\circ$ $z = 9000 \text{ km s}^{-1}$	$z \Delta\alpha > 50, z \Delta\delta > 100, \Delta z \sim 50$

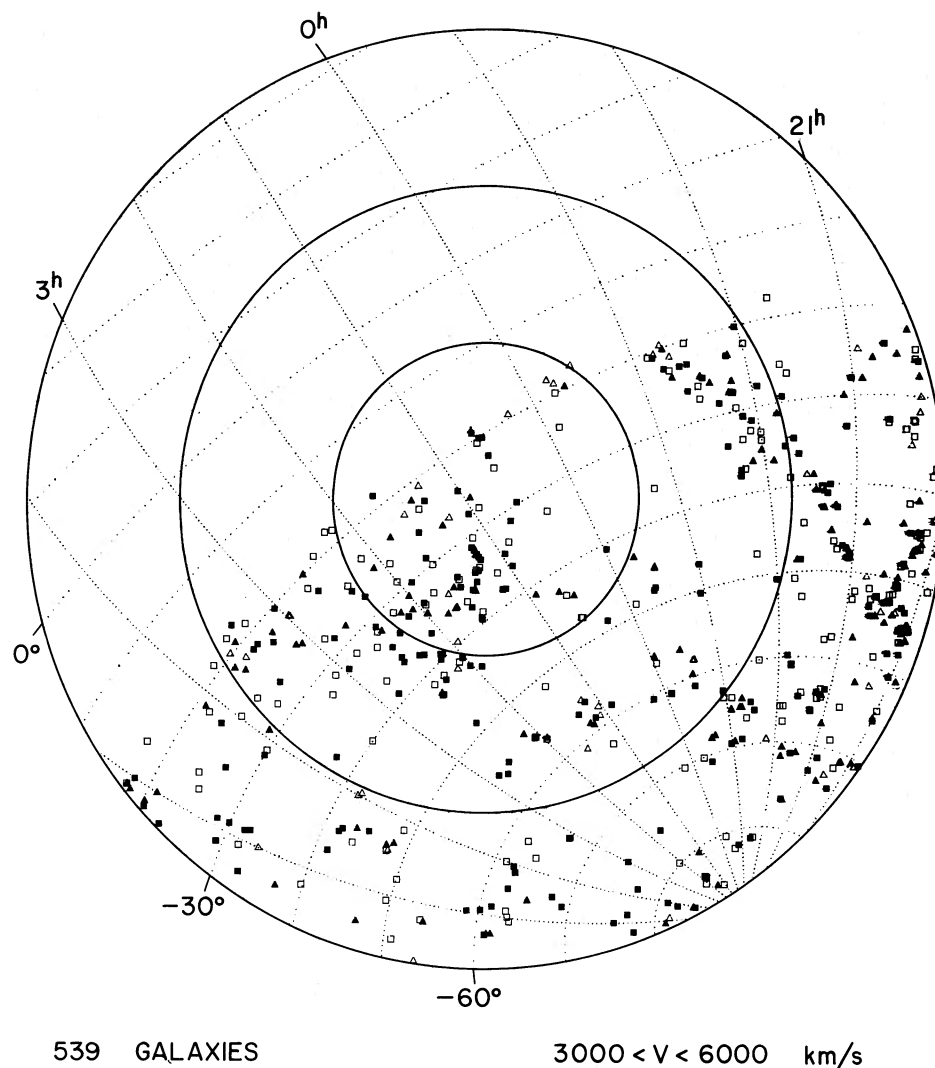


FIG. 6b

the edge of the survey area, however, we cannot from the present data establish its actual shape. The other nearby void mentioned earlier (void 2), in the direction  $\alpha = 21^{\text{h}}$ , is located very close to the western edge of the survey. It is seen in the declination range  $-17.5$  to  $-50^{\circ}$  and has a mean redshift of  $5000 \text{ km s}^{-1}$ . At large distances, there are two other important voids. One (void 3), centered at approximately  $6000 \text{ km s}^{-1}$ , is delineated by two of the structures described above. While it is especially well defined in the declination zone  $-30^{\circ}$  to  $-40^{\circ}$ , it seems to extend farther south, being generally deficient of galaxies up to  $\delta = -60^{\circ}$ . The other (void 4) is at a mean distance of  $9000 \text{ km s}^{-1}$  and spans some  $4000 \text{ km s}^{-1}$  in depth. This empty region is probably the largest in the survey volume, although its backside is undersampled and observations of a deeper sample are necessary to determine its reality and total extent.

#### IV. DISCUSSION

In this paper we have examined the general characteristics of the space distribution of galaxies in the SSRS sample, covering the southern Galactic cap. This sample is the largest existing survey of the southern hemisphere and probes a volume of

space comparable to that of the original CfA redshift survey. Its size and the fact that it covers a distinct region of space make it of particular interest for the purpose of evaluating whether the presently available wide-angle surveys are sufficiently large to represent a fair sample volume of the universe. Comparison between the northern and southern surveys indicates that the clustering morphology of bright galaxies has a reproducible nature and can be considered as fairly well established. Galaxies tend to occupy a small fraction of the surveyed volume, with some fraction of the galaxies forming filaments and sheets which surround empty regions. However, not all galaxies can be neatly assigned to a well-defined large-scale structure; a good fraction of the galaxies are associated in loose groupings that have only the vaguest interconnection to each other.

The space distribution of galaxies described in the previous section can be summarized as consisting of several large structures which divide the survey volume into regions significantly devoid of galaxies. In order to obtain a more easily interpreted projected distribution we show in Figure 8 maps of a part of the galaxy distribution in a Cartesian coordinate system defined in the figure caption. We plot galaxies within contig-

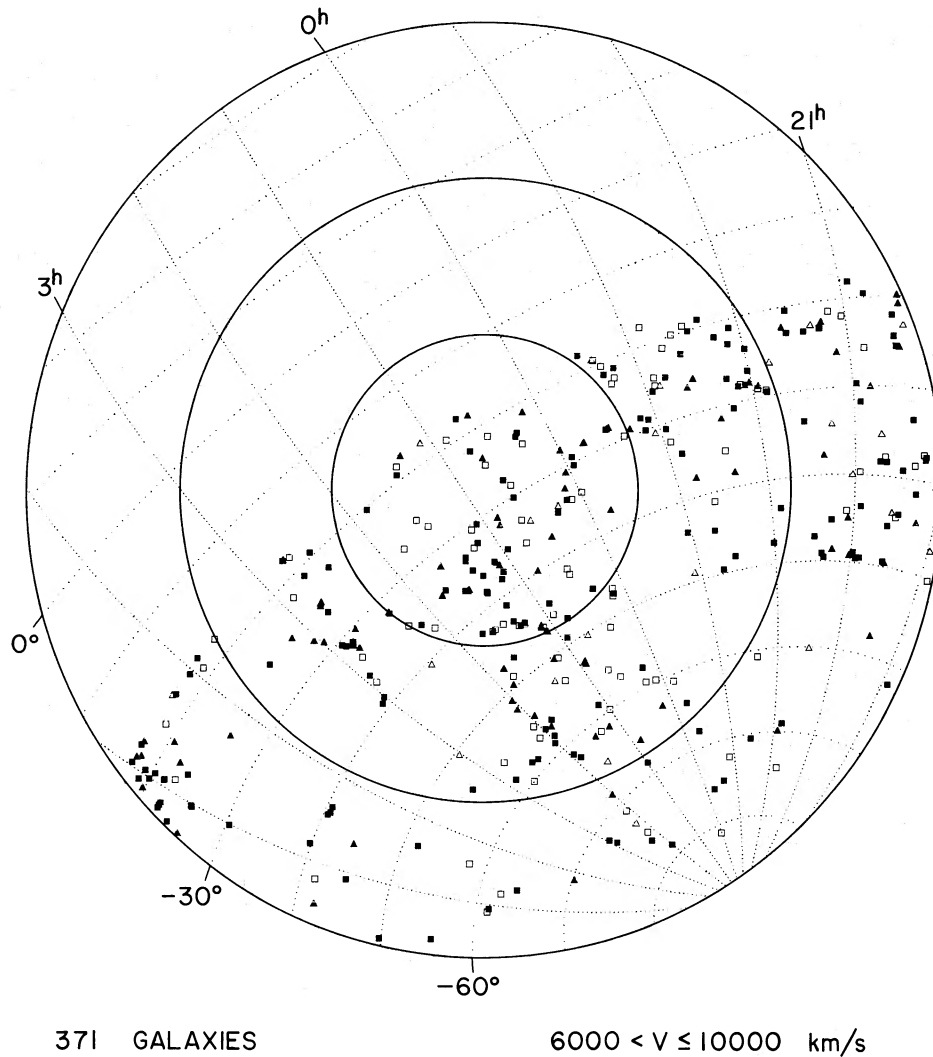


FIG. 6c

uous slabs,  $10 h^{-1}$  Mpc thick, in the region of the survey encompassing the largest volume. The shape and extent of the main structures observed are not well-defined, because of selection and boundary effects. However, examination of the distribution in the Cartesian system suggests that the structure in the eastern side of the survey ( $x < 0$ ), the “wall” at a mean distance of  $50 h^{-1}$  Mpc, is primarily planar within the observed volume. It can be described by the simple expression  $y = 2x = 80$ , independent of  $z$ , in units of  $h^{-1}$  Mpc. It extends to the limit of the survey area for at least  $50 h^{-1}$  Mpc in depth,  $30 h^{-1}$  Mpc in the observed declination range and has a typical thickness of  $5 h^{-1}$  to  $10 h^{-1}$  Mpc. The second major component, lying in the Telescopium-Pavo-Indus (T-P-I) region, is a more complex conglomerate of condensed substructures. While it is actually formed by several small groups, it still appears to form a connected two-dimensional structure, extending as much as  $60 h^{-1}$  Mpc in depth and with a transverse dimension of over  $40 h^{-1}$  Mpc. The “wall,” on the other hand, has much less pronounced substructure, especially as seen in the wedge plots. Inspection of the projection maps in the Cartesian system reveals that the T-P-I complex intersects another sheet at a sharp angle, which is not very well mapped

since it is located at the western edge of the survey. It is interesting that in Figure 8 this branch of the Telescopium-Pavo-Indus complex appears even more prominent than that observed in the wedge diagrams. This illustrates the basic difficulty of grasping the characteristics of a three-dimensional distribution from a set of projection maps.

The wedge diagrams and the Cartesian map give clear evidence of a “bridge,” at a mean distance of  $30 h^{-1}$  Mpc and  $30 h^{-1}$  Mpc long, connecting the “wall” and the T-P-I complex and forming the front side of void 3. A preliminary attempt to analyze the distribution taking into account the selection effects suggests that the backside edge of this void occurs within the survey volume and bridges the major structures at larger distances, but this must be confirmed by deeper samples. Besides all these structures, the maps examined also show several less prominent, sometimes curved, filaments which intersect the larger sheets often forming sharp edges. These curved structures closely resemble those described by de Lapparent, Geller, and Huchra (1986) who described the overall galaxy distribution in terms of bubbles in contact.

In the preceding section we have attempted to identify individual voids on the basis of visual inspection of the several

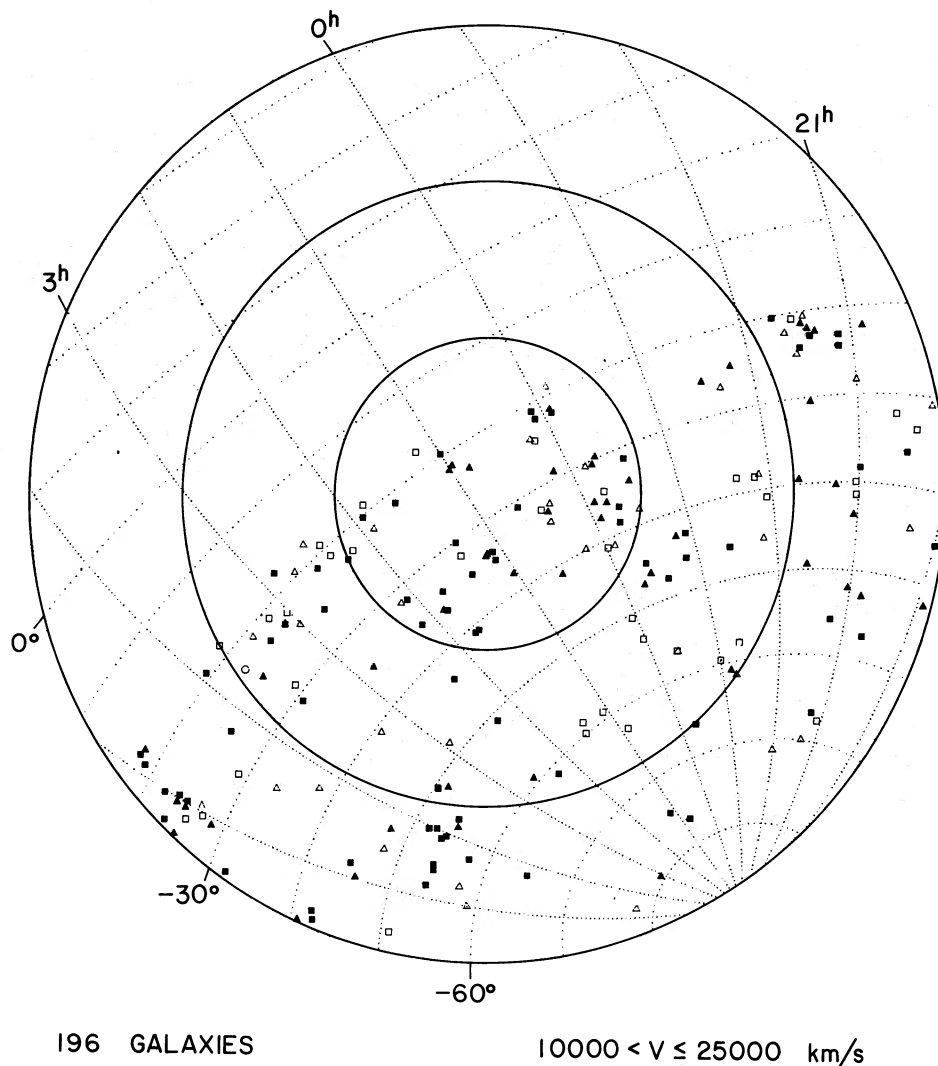


FIG. 6d

projection maps presented. We have called attention to at least four relative prominent empty regions, with typical sizes ranging from  $10 h^{-1}$  to  $60 h^{-1}$  Mpc. Although we have described them as separate entities, the voids do not seem to be completely surrounded by unbroken sheets as would a bubble, but rather they appear to be connected throughout the survey volume, giving the impression of a spongy topology as described by Gott, Melott, and Dickinson (1986). It is also significant that the voids seem to be deficient in all types of galaxies, including the dwarf galaxies. This is a qualitative statement that will be supplemented with detailed correlation analyses in a future paper. One of the voids (void 1) identified here is particularly interesting for further investigating this question due to its proximity.

The above description is rather qualitative and meant solely to highlight some of the prominent features of the observed galaxy distribution. However, the fact that the clustering pattern of bright galaxies has been confirmed to have a reproducible appearance is, by itself, already important, since it imposes stringent constraints on theoretical models. Successful models for the formation and evolution of large-scale structures must be able to reproduce at least the major features of

the observed distribution described here. In this respect, it is remarkable that the observed distribution in the south looks very similar in nature to the results of the  $N$ -body simulations of White *et al.* (1987) in a flat, cold, dark matter model of the universe. For example, their Figure 10 bears a striking resemblance to our Figures 7a–c, especially in the nature of the long diagonal filaments. In future papers we intend to investigate the properties of the SSRS using the different quantitative methods that have been developed to analyze several recent surveys. A quantitative description of the properties of the observed distribution is essential to allow the comparison with results of White *et al.* (1987) and other numerical simulations. We hope that from this comparison we may eventually be able to discriminate among the competing models that have been proposed to account for the formation of large-scale structure in the universe.

Several people have contributed to the survey and we thank them all for their support. L. N. da Costa and P. S. Pellegrini would like to thank J. Geary and M. A. Nunes for keeping the ON detector running over the years and C. Willmer, R. de

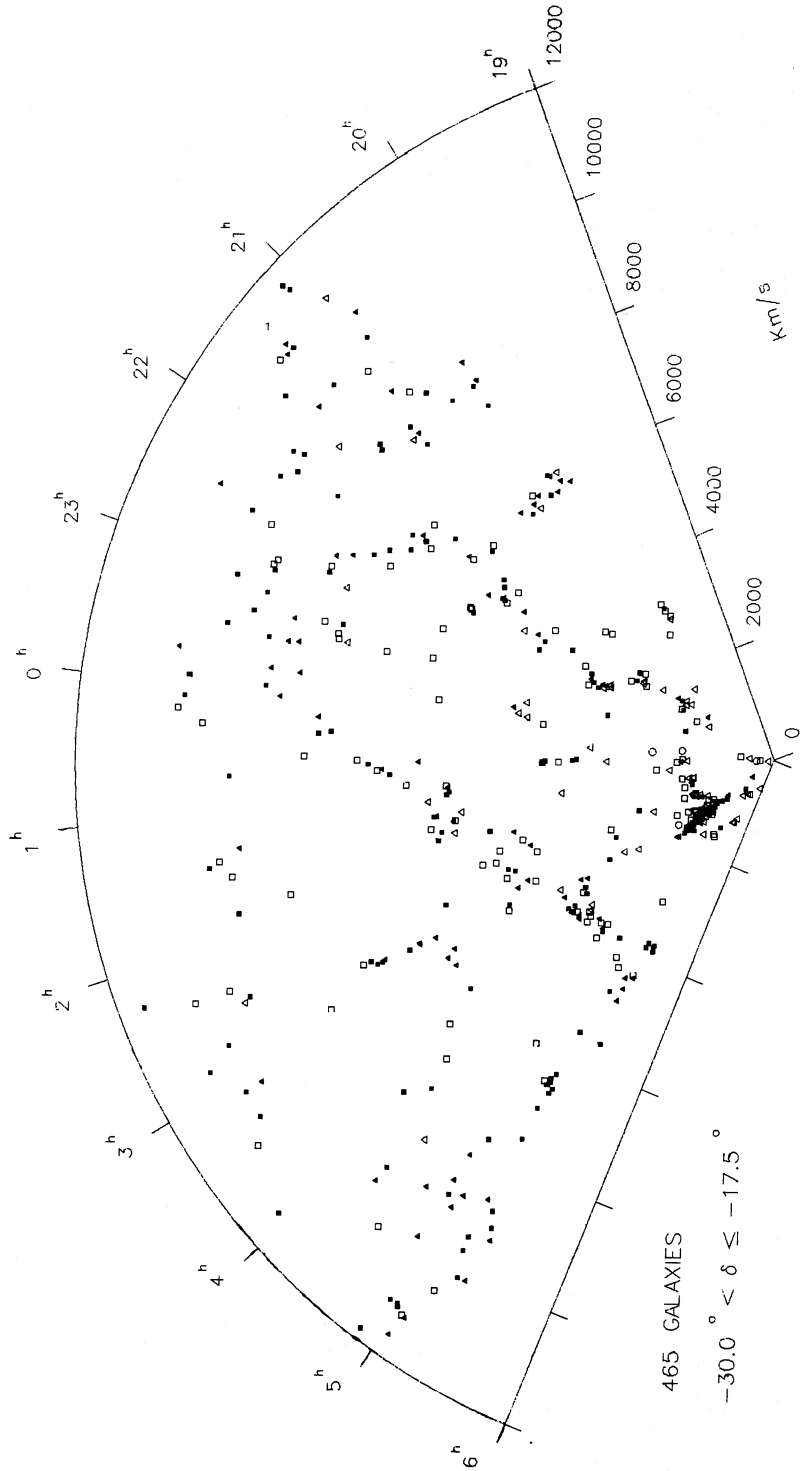
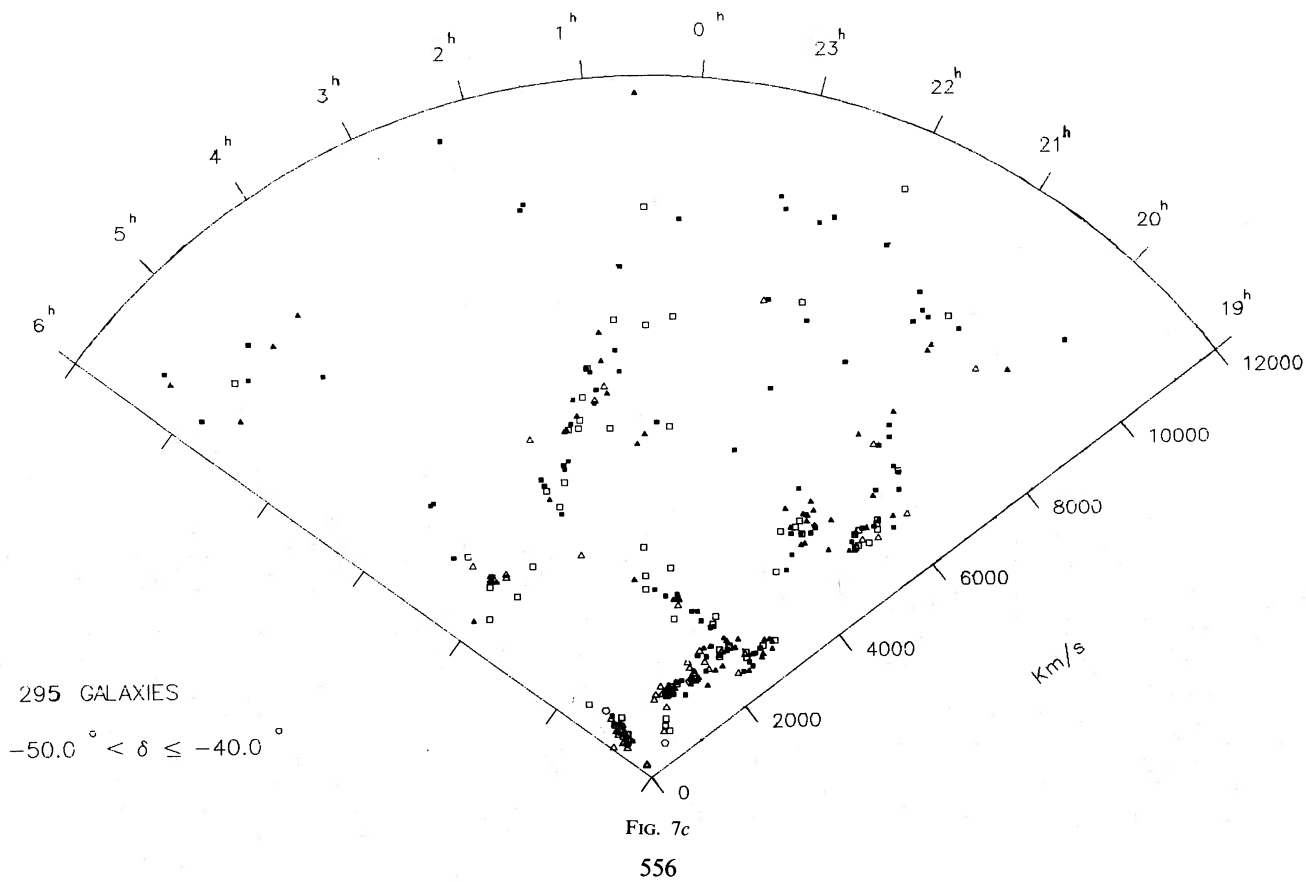
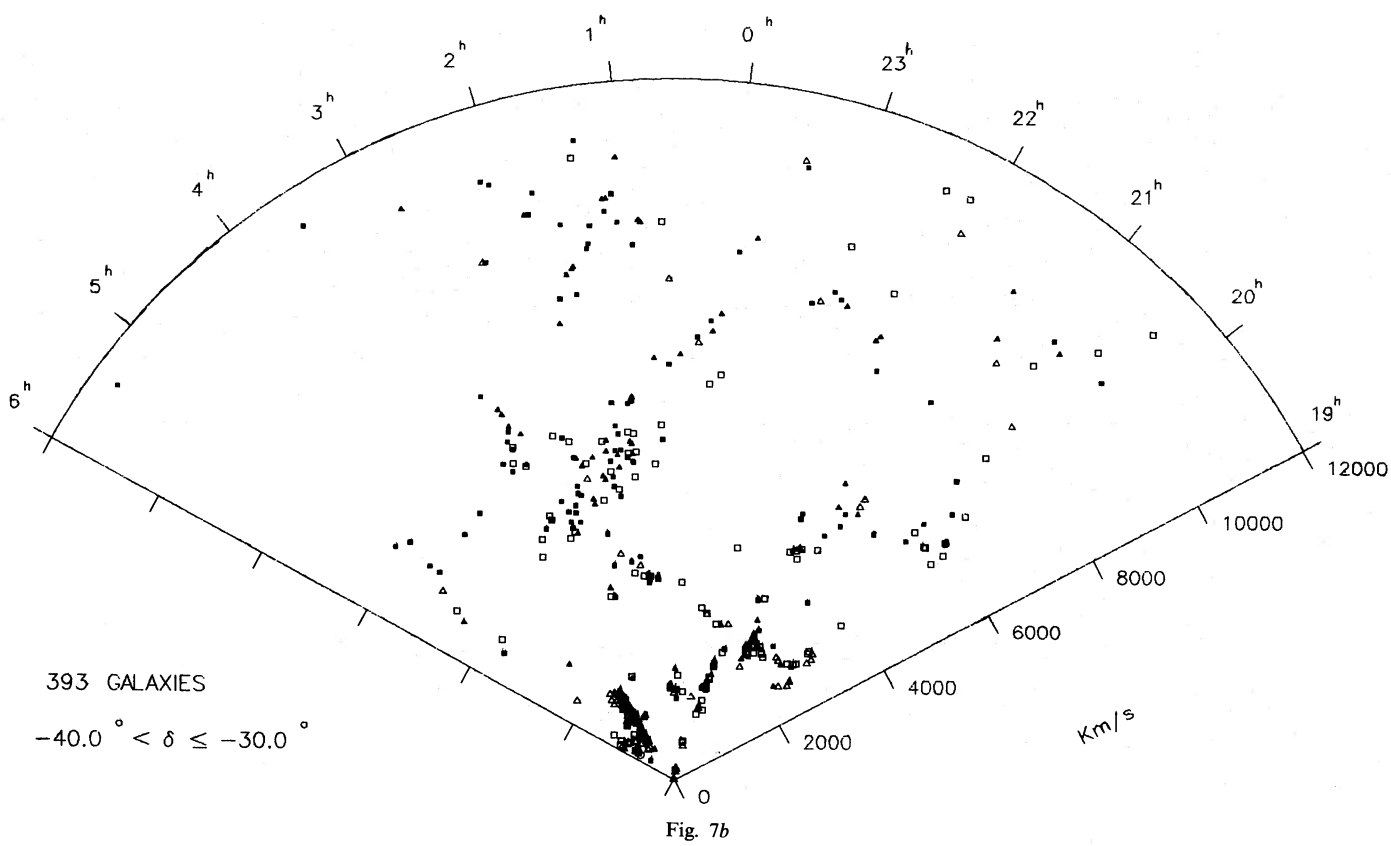


FIG. 7a

FIG. 7.—Cone diagrams of right ascension vs. redshift showing galaxies in the SSRS sample with  $v < 12,000 \text{ km s}^{-1}$ . The range in declination of each wedge is indicated in the figures. The symbols are the same as in Fig. 6.



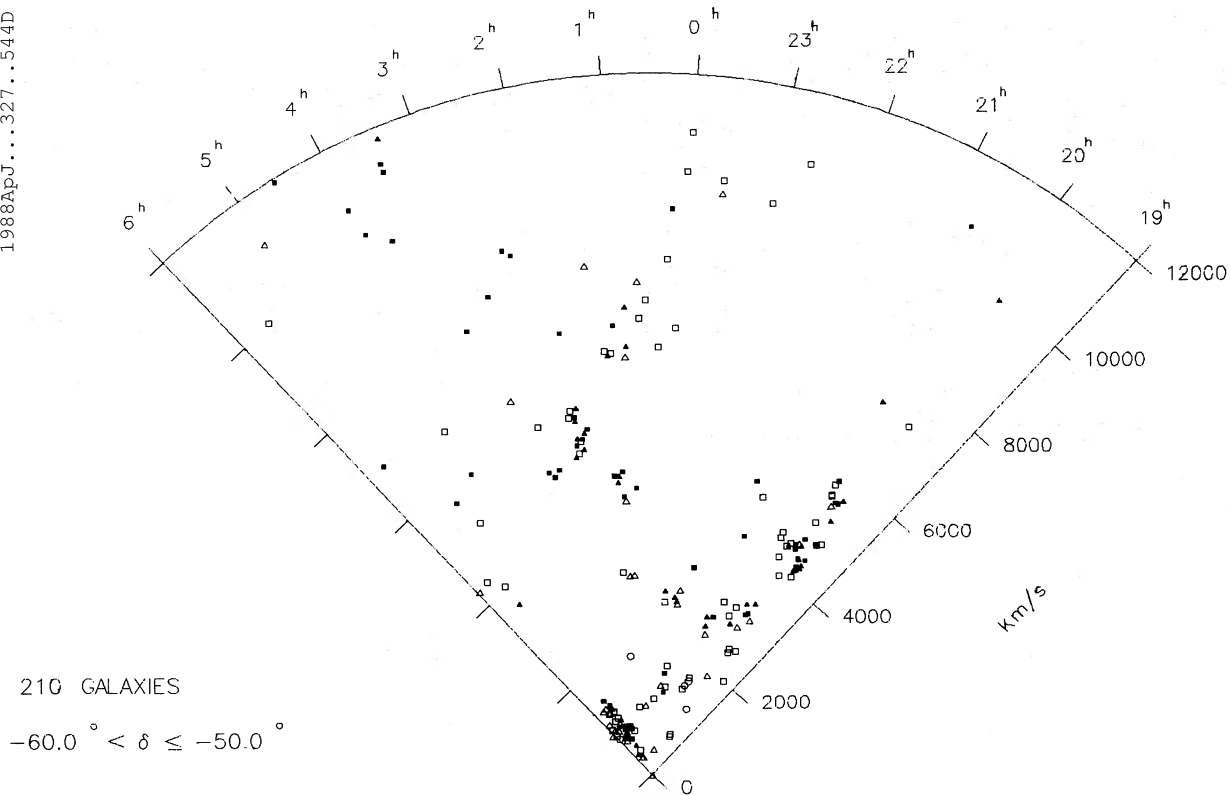


FIG. 7d

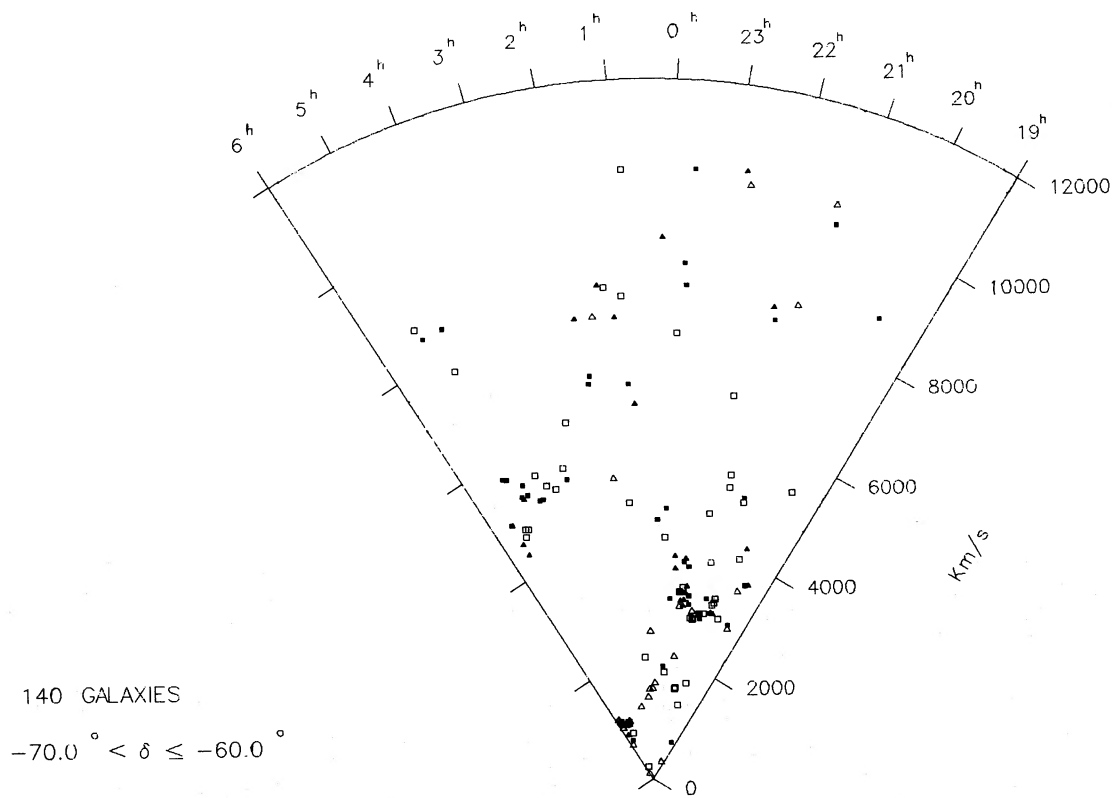


FIG. 7e

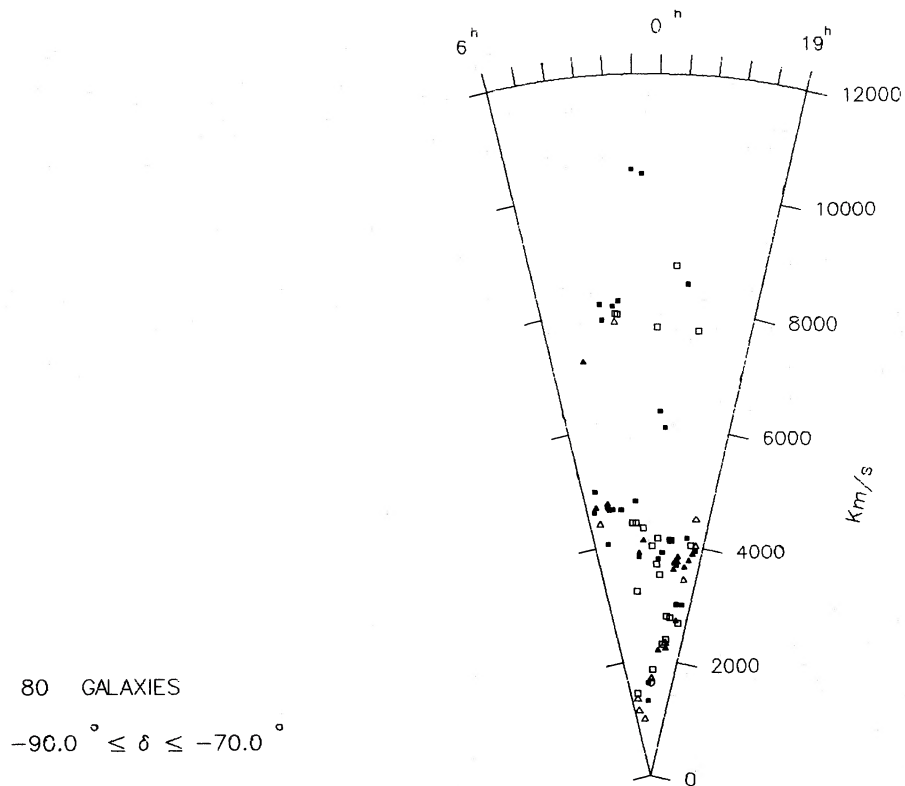


FIG. 7f

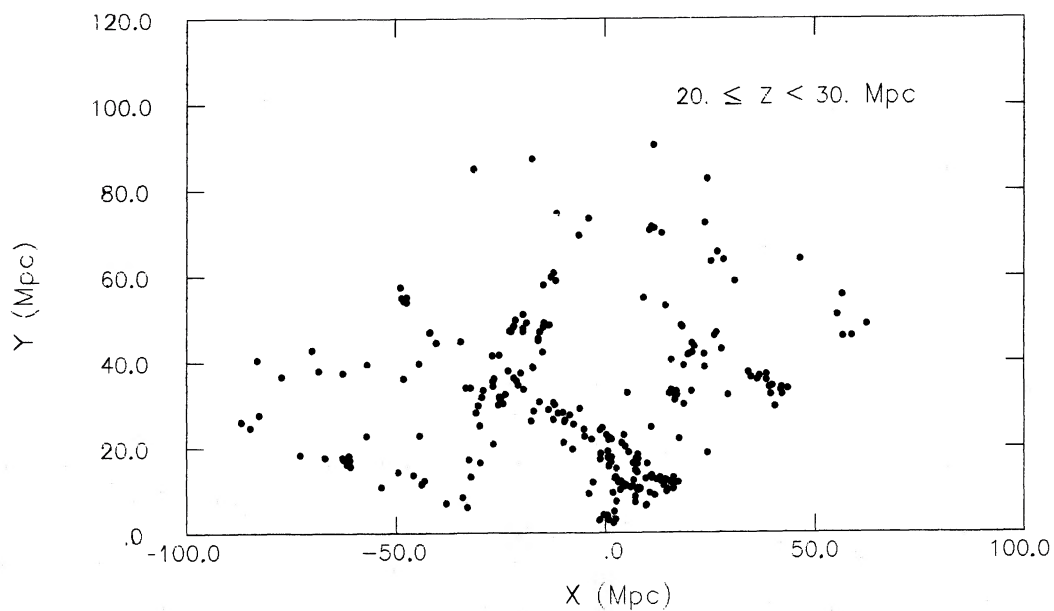


FIG. 8a

FIG. 8.—Distribution of galaxies plotted in a Cartesian coordinate system with the  $x$  and  $y$  axes lying in the equatorial plane and pointing in the directions of  $\alpha = 18^h$  and  $\alpha = 0^h$ , respectively; the  $z$  axis toward the south celestial pole. In the figure we show the projection onto the  $(x - y)$ -plane of galaxies with  $v < 10,000 \text{ km s}^{-1}$  covering the range  $20 < z < 50 \text{ h}^{-1} \text{ Mpc}$ , in  $10 \text{ h}^{-1} \text{ Mpc}$  intervals.

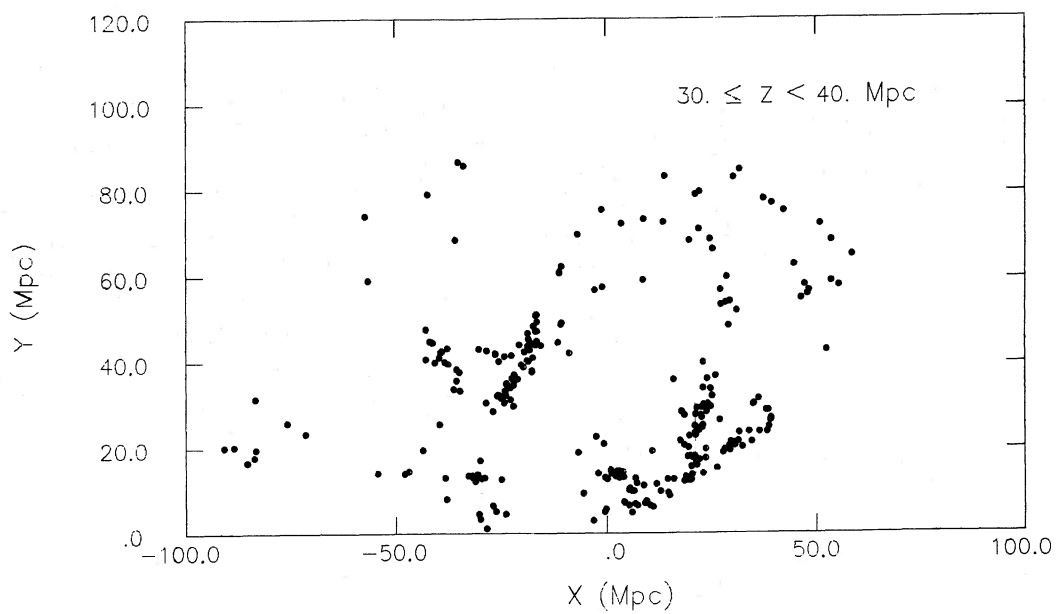


FIG. 8b

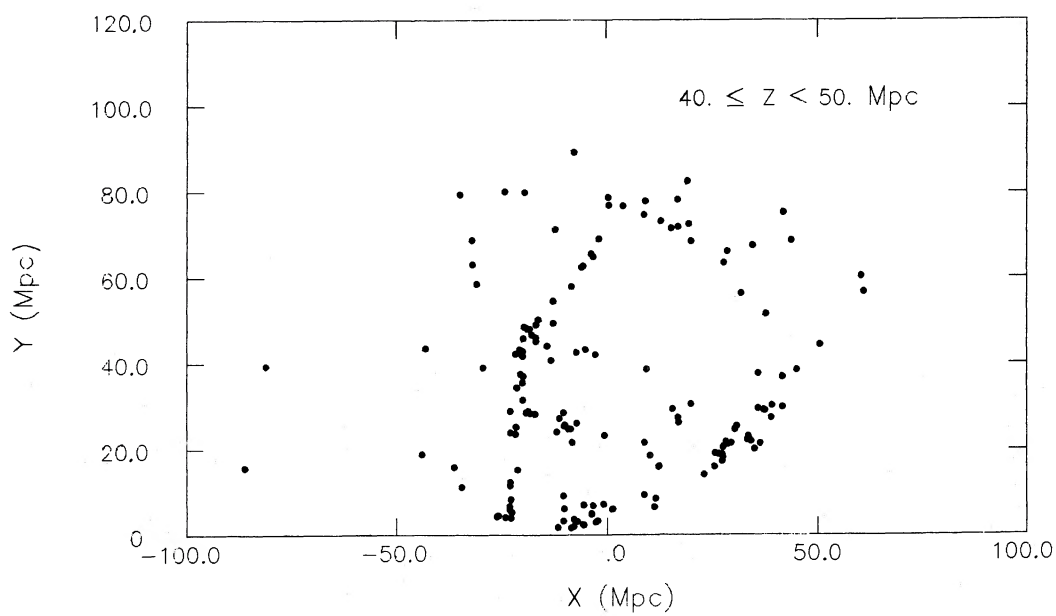


Fig. 8c

Carvalho, M. Maia, C. Rite, D. Nascimento, B. Wyatt, G. Madjeski, and L. Feldman for their contribution in various stages of this project. We also acknowledge help from

C. Steidel, C. Hassler, and V. Lindsay. W. L. W. Sargent and M. Davis received support from NSF under grants AST-8416704 and AST-8614552, respectively.

## REFERENCES

- da Costa, L. N., Pellegrini, P. S., Nunes, M. A., Willmer, C., and Latham, D. W. 1984, *A.J.*, **89**, 1310.  
 Davis, M., and Geller, M. 1976, *Ap. J.*, **208**, 13.  
 Davis, M., and Huchra, J. 1982, *Ap. J.*, **254**, 437 (DH).  
 Davis, M., Huchra, J., Latham, D., and Tonry, J. 1982, *Ap. J.*, **253**, 423.  
 de Lapparent, V., Geller, M., and Huchra, J. P. 1986, *Ap. J. (Letters)*, **302**, L1.  
 de Vaucouleurs, G. 1975, in *Galaxies and the Universe*, ed. A. Sandage, M. Sandage, and J. Kristian (Chicago: University of Chicago Press), p. 557.  
 de Vaucouleurs, G., de Vaucouleurs, A., and Corwin, H. 1976, *Second Reference Catalog of Bright Galaxies* (Austin: University of Texas Press) (RC2).  
 Gott, J. R., Melott, A. L., and Dickinson, M. 1986, *Ap. J.*, **306**, 341.  
 Haynes, M. P., and Giovanelli, R. 1986, *Ap. J. (Letters)*, **306**, L55.  
 Huchra, J. P., and Geller, M. 1982, *Ap. J.*, **257**, 423.  
 Huchra, J. P. and Geller, M. 1987, to appear in "The Proceedings of the 13th Texas Symposium on Relativistic Astrophysics", ed. M. Ulmer, (Singapore: World Scientific) p. 275.  
 Huchra, J. P., Davis, M., Latham, D., and Tonry, J. 1983, *Ap. J. Suppl.*, **52**, 89.  
 Kaiser, N. 1987, *M.N.R.A.S.*, **227**, 1.  
 Lauberts, A. 1982, *The ESO/Uppsala Survey of the ESO(B) Atlas* (München: European Southern Observatory).  
 Menzies, J. W., Coulson, I. M., and Sargent, W. L. W. 1987, *A.J.*, in print.  
 Nilson, P. 1973, *Uppsala General Catalog of Galaxies (Uppsala Astr. Obs. Ann.* **6**).  
 Ostriker, J. P., and Cowie, L. L. 1981, *Ap. J. (Letters)*, **243**, L127.  
 Ostriker, J. P., Thompson, C., and Witten, E. 1986, *Phys. Letters B*, **180**, 231.  
 Sandage, A. 1975, *Ap. J.*, **202**, 563.  
 Sargent, W., Tonry, J., da Costa, L., Pellegrini, P. S., Davis, M., Meiksin, A., and Latham, D. 1987, in preparation.  
 White, S. D. M., Frenk, C. S., Davis, M., and Efstathiou, G. 1987, *Ap. J.*, **313**, 505.

I. A. COULSON and J. W. MENZIES: South African Astrophysical Observatory, P.O. Box 9, Observatory 7935, South Africa

L. NICOLACI DA COSTA and P. S. PELLEGRINI: CNPq/Observatorio Nacional, Rua General Bruce 586, Sao Cristovao, 20921, Rio de Janeiro, Brasil

MARC DAVIS and AVERY MEIKSIN: Department of Astronomy, University of California at Berkeley, Berkeley, CA 94720

DAVID W. LATHAM: Center for Astrophysics, 60 Garden Street, Cambridge, MA 02138

W. L. W. SARGENT: Department of Astronomy 105-24, California Institute of Technology, Pasadena, CA 91125

JOHN L. TONRY: Department of Physics 37-521, Massachusetts Institute of Technology, Cambridge, MA 02139